Journal of Scientific Research & Reports

27(6): 119-137, 2021; Article no.JSRR.70535
ISSN: 2320-0227

Reservoir Simulation Analysis of Pressure Depletion Performance in Gas-Condensate Reservoirs: Black-Oil and Compositional Approaches

Akinsete O. Oluwatoyin[1*] and Anuka A. Agnes[1,2]

[1]Department of Petroleum Engineering, University of Ibadan, Ibadan, Nigeria.
[2]Department of Petroleum Engineering, University of Calabar, Calabar, Nigeria.

Authors' contributions

This work was carried out in collaboration between both authors. Both authors read and approved the final manuscript.

Article Information

DOI: 10.9734/JSRR/2021/v27i630406
Editor(s):
(1) Dr. Ozlem Sultan Aslanturk, Adnan Menderes University, Turkey.
Reviewers:
(1) Achide Samson Achide, Nigeria.
(2) Ariffin Samsuri, Universiti Teknologi Malaysia, Malaysia.
Complete Peer review History: https://www.sdiarticle4.com/review-history/70535

Original Research Article

Received 01 May 2021
Accepted 08 July 2021
Published 28 July 2021

ABSTRACT

Pressure depletion in gas-condensate reservoirs create two-phase flow. It is pertinent to understand the behavior of gas-condensate reservoirs as pressure decline in order to develop proper producing strategies that would increase gas and condensate productivity.

Eclipse 300 was used to simulate gas-condensate reservoirs, a base case model was created using both black-oil and compositional models. The effects of three Equation of States (EOS) incorporated into the models were analysed and condensate dropout effect on relative permeability was studied.

Analysis of various case models showed that, gas production was maintained at 500MMSCF/D for about 18 and 12 months for black-oil and compositional models, respectively. However, the compositional model revealed that condensate production began after a period of two months at 50MSTB/D whereas for the black oil model, condensate production began immediately at 32MSTB/D. Comparison of Peng-Robinson EOS, Soave-Redlich-Kwong EOS and Schmidt Wenzel EOS gave total estimates of condensate production as 19MMSTB, 15MMSTB and 9MMSTB and initial values of gas productivity index as 320, 380 and 560, respectively. The results also showed that as condensate saturation increased, the relative permeability of gas decreased from 1 to 0 while the relative permeability of oil increased from 0.15 to 0.85.

**Corresponding author: E-mail: oo.akinsete@ui.edu.ng;*

The reservoir simulation results showed that compositional model is better than black-oil model in modelling for gas-condensate reservoirs. Optimal production was obtained using 3-parameter Peng-Robinson and Soave-Redlich-Kwong EOS which provide a molar volume shift to prevent an underestimation of liquid density and saturations. Phase behaviour and relative permeability affect the behaviour of gas-condensate reservoirs.

Keywords: Gas reservoir; gas-condensate reservoir; equation of states; reservoir simulation.

1. INTRODUCTION

Gas-condensate reservoirs are often encountered in most gas reservoir assets globally and have become a major trend of focus for the energy industry in recent times. According to Ifeanyi and his co-worker [1], efficient and cost-effective reservoir management of gas-condensate reservoirs requires meeting the unique accurate well deliverability and liquid recovery predictions challenges posed by these assets.

The factors contributing to optimum development strategy of condensate recovery are the: phase behaviour, relative permeability and production scheme. These factors are also liable for the damage of well deliverability near the wellbore, hence, safe modelling of flow behaviour will address this deliverability problem. Well producing scheme may impose significant influence on the phase behaviour i.e. pressure depletion creates two phase flow which impacts reservoir performance [2,3]. In 2017, Ifeanyi and co-researcher [1] in their work showed that heavier hydrocarbon components in the gas, during the production of a gas-condensate reservoir, drop out as liquid as reservoir pressure drops below the fluid dew point pressure. The constant compositional changes in the gas condensate reservoir, makes it a complex system thereby requiring compositional simulation to be able to model the phase behavior of the fluid and evaluate the recovery processes properly [4].

The main objective of the work described in this paper therefore is to: predict the performance of a gas condensate reservoir; study the effect of the two parameter and three parameter equations of state in predicting the performance of a gas condensate reservoir and determine the effect on relative permeability and well deliverability of pressure depletion in a gas condensate reservoir.

2. GAS-CONDENSATE PRODUCTION

Gas-condensates are single-phase gaseous hydrocarbon in the reservoir with considerable liquid hydrocarbon content dissolved in them at a particular reservoir condition. Gas-condensate production is mainly gas from which more or less liquid is condensed in the surface separators, hence the name gas-condensate [5]. Isothermal production of the reservoir results in an attendant pressure decline which if not controlled in a condensate system, will drop beyond the dew point with the emergence of a two-phase scenario. The heavier fractions of the previously single phase fluid begin to condense out at this point [6]. This retrograde condensate formation results in build-up of a liquid phase around the wellbore, leading to a decrease in the effective permeability to gas into the wellbore.

3. PROPERTIES OF GAS CONDENSATE FLUIDS

3.1 Behaviour of Gas Condensate Fluids

A gas condensate is a single-phase fluid at original reservoir conditions. It consists predominantly of methane (C_1) and other short-chain hydrocarbons, but it also contains long chain hydrocarbons, termed heavy ends. Under certain conditions of temperature and pressure, this fluid will separate into two phases, a gas and a liquid that is called a retrograde condensate.

As reservoir is being produced, formation temperature usually doesn’t change, but pressure decreases. The largest pressure drops occur near producing wells. When the pressure in a gas-condensate reservoir decreases to a certain point, called the saturation pressure or dew point, liquid phase rich in heavy ends drops out of solution; the gas phase is slightly depleted of heavy ends. A continued decrease in pressure increases the volume of the liquid phase up to a maximum amount; liquid volume then decreases. This behaviour can be displayed in a pressure-volume-temperature (PVT) diagram (Fig. 1).

3.2 Phase Envelope of Gas-condensate Fluids

The phase envelope of a gas-condensate has a critical temperature less than the reservoir temperature and a cricondentherm greater than the reservoir temperature [9]. In gas-condensate phase envelope (Fig. 2), the reservoir temperature lies between the critical point temperature and the cricondentherm. Initially, the fluid in the reservoir consists of a single vapour phase, as the reservoir is depleted, the vapour expands until the dew point line is reached, after which increasing amounts of liquid are condensed from the vapour phase [8]. Forecasting and production analysis of a gas condensate reservoir is difficult due to this complex multiphase behaviour; a portion of gas with heavier hydrocarbons condenses out and gets trapped in the subsurface porous network. This process is called the isothermal retrograde condensation; as pure substances are expected to evaporate when pressure is reduced. Such condensation could be significant near the wellbore due to the large drop in pressure compared to the reservoir [8,10].

The major characteristic feature of a gas condensate fluid is the Gas-Oil Ratio (GOR). The condensate fluid can be further classified into four categories: Lean, medium, rich and very rich condensate. As the isothermal condition of the reservoir fluid approaches the critical point, in the phase envelope, the richness of the fluid is increased (Fig. 3).

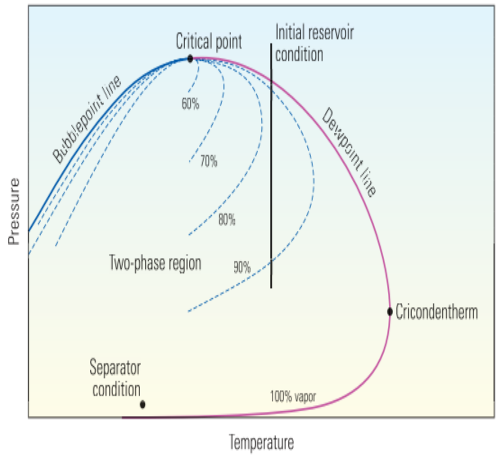

Fig. 1. Phase diagram of a gas condensate system (Source: Fan et al., 2005) [7]

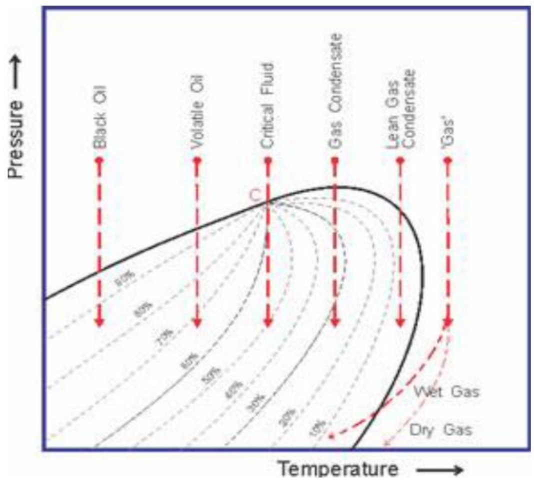

Fig. 2. Phase envelope of a gas condensate reservoir (Source: Aaditya, 2014) [8]

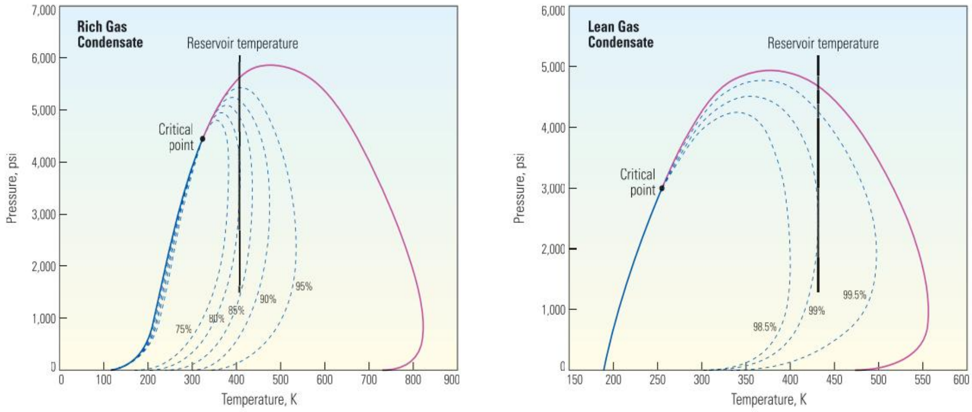

Fig. 3. Rich and Lean Gas Condensate Behaviour (Source: Akpabio et al., 2015) [4]

3.3 Condensate Blockage

Gas condensates exhibit complex phase and flow behaviours due to the appearance of condensate liquid when the bottom-hole pressure drops below the dew point pressure. The accumulated condensate in the vicinity of the wellbore causes a blockage effect and reduces the effective permeability appreciably, depending on a number of reservoir and well parameters, and also causes the loss of heavy components at surface [1].

Condensate blockage is one of the major problems that have been addressed in the industry [10,11,12,13]. As reservoir fluid pressure declines below the dew point pressure during the production process, the liquid drops out of the gas phase and forms condensate in the formation. There are two scenarios that can result in a pressure drop. The first one is the pressure drop due to the flow of the reservoir fluid. The reservoir fluid flows from a high pressure of the reservoir to a lower pressure of the separators at the surface. The second scenario is the drop in reservoir pressure due to pressure depletion. During the production of gas and condensate, the reservoir pressure will decrease with time and when it drops below the dew point pressure, condensate forms everywhere inside the reservoir, as condensate increases gas permeability decreases [14]. A key factor that controls the gas-condensate well deliverability is the relative permeability, which is influenced directly by the condensate accumulation. The accumulated condensate bank not only reduces both the gas and liquid relative permeability, but also changes the phase composition of the reservoir fluid, hence reshapes the phase diagram of reservoir fluid and varies the fluid properties [10]. The impact of condensate blockage is very sensitive to the gas and oil relative permeabilities in the region around the wellbore. Several laboratory experiments [10,12,15] have demonstrated an increase in mobility for gas-condensate fluids at the high velocities typical of the near-well region, a mechanism that would reduce the negative impact of condensate blockage.

4. THREE REGION THEORY

As the average pressure in a gas-condensate reservoir continues to decline on production, condensate dropout occurs across the reservoir. In 2003, Rajeev [16] gave an accurate yet simple model of a gas condensate well undergoing depletion which consists of three flow regions (Fig. 4).

• **Single-Phase Gas Region 3**: This is a region that is far away from the well and has reservoir pressure higher than the dew point, and hence only contains single phase gas [15]. This third region includes most of the reservoir away from the producing wells. Since it is above the dew point pressure, there is only one hydrocarbon phase (which is gas) present and flowing. The interior boundary of this region is not stationary, but moves outward as hydrocarbons are produced from the well and the formation pressure drops, eventually disappearing as the outer-boundary pressure drops below the dew point [7].

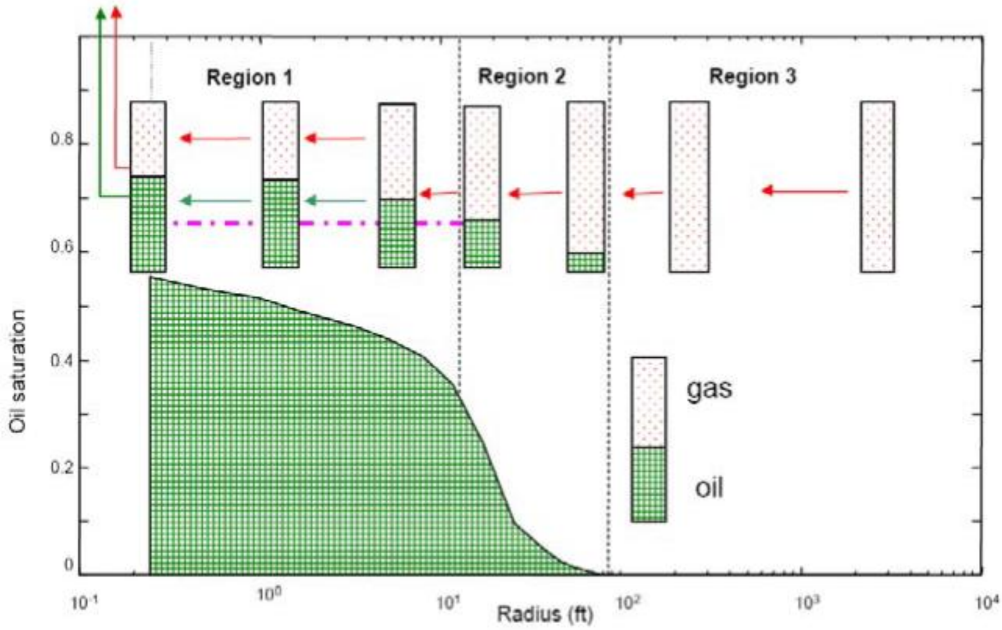

Fig. 4. Schematic gas condensate flow in three regions [15]

• **Condensate build-up Region 2**: In this region reservoir pressure drops below the dew point, and condensate drops out in the reservoir. Though, the accumulated condensate saturation is not high enough for the liquid phase to flow. The accumulation of condensate is not sufficient to be mobile because it has not reached the critical condensate saturation [15]. As the condensate build-up occurs in Region 2, a short period of transition time is needed to build up Region 1. The condensate build-up is mainly caused by: the bulk volume depletion of the reservoir and the pressure gradient imposed on the flowing reservoir gas within Region 2. If the build-up of condensate is caused by the pure pressure depletion, the condensate saturation is calculated from the liquid dropout curve from a constant volume depletion (CVD) experiment corrected for water saturation [17].

• **Near Well Region 1**: Here reservoir pressure drops further below the dew point, the critical condensate saturation is exceeded, and part of the condensate build-up becomes mobile. The mobility of the gas phase is greatly impaired due to the existence of the liquid phase [15]. The condensate blockage mainly occurs in Region 1 because condensate impairment restricts the flow of gas to the well. Depending on the richness of the gas-condensate the relative permeabilities of gas and condensate change as a function of time and the pressure in Region 1 contributes to condensate blockage. The existence of condensate blockage region will vary depending on richness of the gas-condensate. In rich gas-condensate reservoirs, condensate blockage is an important phenomenon because of the highest liquid dropout which in turn serves as condensate impairment to the gas flow [17].

4.1 Pressure and Temperature Ranges of Gas-Condensate Reservoirs

According to Bradley et al. [18] pressures and temperatures of retrograde gas-condensate reservoirs are in the range of 3,000 to 8,000 psi and 200 to 400°F, respectively. These pressure and temperature ranges, together with wide composition ranges, provide a great variety of conditions for the physical behaviour of gas condensate deposits. Pressure depletion in gas-condensate reservoir can be modelled in the laboratory using constant volume depletion and constant composition expansion tests; also by various correlation [18,19].

4.2 Constant Volume Depletion Test

During the CVD test, pressure is decreased at regular intervals by releasing small amounts of gas from a pressurized gas sample while keeping the volume of gas in the cell constant, thereby emulating the behaviour of producing gas reservoirs. The main objective of this test is to measure the relative volume of liquid condensing (liquid saturation or liquid dropout) from natural gas as the field pressure declines. Results of this test give operators an estimate of the condensates/gas ratio and the volumes of liquids that need to be handled by surface production facilities for the field [10,20].

4.3 Constant Composition (mass) Expansion Test

The constant composition expansion (CCE) test, sometimes referred to as a constant-mass expansion test, is used to measure dew point pressure, single-phase gas compressibility factor, and oil relative volume below the dew point [10]. A sample of reservoir fluid is charged in a visual PVT cell and brought to reservoir temperature and a pressure sufficiently high to ensure single-phase conditions. Pressure is lowered by increasing cell volume until a liquid phase is visually detected (through a glass window). Total cell volume and liquid volume are monitored from the initial reservoir pressure down to a low pressure [10,21].

4.4 Modelling Condensate Blockage

Reservoir simulation models [22,23,24,25] are commonly used to predict the performance of gas-condensate reservoirs. Study has shown that coarse grid model may significantly overestimate well deliverability, hence, the most accurate way to determine near well behaviour of a gas-condensate reservoir is by using a simulator with a fine grid [7]. To accurately model gas-condensate fluid behaviour and capture condensate banking phenomena in the vicinity of the well, it is proper to select reasonable grid block size. It is stated by Fevang et al. [26] that the multiphase pseudo pressure method treats the more important Region 1 accurately in coarse grid simulation. They also claimed that the size of the well grid-cell must be chosen properly in order not to overestimate pressure losses in Region 1.

The comparison of the Modified Black-Oil (MBO) and compositional approach in full-field simulation studies was made in some papers. According to Ahmed et al. [27] the MBO approach proved to be sufficient for modelling gas-condensate behaviour below the dew point and instead of using a fully compositional approach. It was proposed by Fevang et al. [26] that a modified oil viscosity should be used in Black-Oil model in order to obtain the same result as a full compositional model [17].

4.5 Equations of State

An Equation of State (EOS) is a semi-empirical functional relationship between pressure, volume and temperature of a pure substance. It is a thermodynamic equation describing the state of matter under a given set of physical conditions [28]. According to Duan and Hu [29] EOS is the relationship between the Pressures (*P*), Temperatures (*T*), Volumes (*V*) and Compositions(*x*) of components, used to compute various thermodynamic properties. It represents the phase behavior of the fluid, both in the two-phase envelope (that is, inside the binodal curve), on the two-phase envelope, and outside the binodal curve.

Numerous EOS have been proposed to represent the phase behavior of pure substances and mixtures in the gas and liquid states since van der Waals [30] introduced his expression in 1873. These equations were generally developed for pure fluids and then extended to mixtures through the use of mixing rules [31]. The van der Waals EOS was the first equation to predict vapor-liquid coexistence [28]. Later, the Redlich-Kwong EOS [31] improved the accuracy of the van der Waals equation by introducing temperature-dependence for the attractive term. Soave [32] and Peng and Robinson [33] proposed additional modifications to more accurately predict the vapor pressure, liquid density, and equilibria ratios. Other authors [34,35,36] in the late twentieth century modified the repulsive term of the van der Waals EOS to obtain accurate expressions for hard body repulsion; while according to Wei and Sadus [37] both the attractive and repulsive terms of the van der Waals EOS was modified by Chen and Kreglewski [38], Christoforakos and Franck [39] and Heilig and Franck [40].

In 1972, Soave [32] proposed an important modification to the Redlich-Kwong Equation of State (EOS), his modification fitted experimental vapor-liquid data well and could predict phase behavior of mixtures in the critical region. Until the work of Soave (1972), modifications to the van der waals EOS focused on temperature dependency of the attractive parameter [28]. The Soave-Redlich-Kwong EOS (equations 1-2) has become the most popular equation of state for natural gas systems in the petroleum industry.

$$P = \frac{RT}{v-b} - \frac{a(T)}{v(v+b)} \quad (1)$$

Where

$$a(T) = 0.42747\frac{R^2T_c^2}{P_c}\alpha(T) \quad (2)$$

$$b = 0.0867\frac{RT_c}{P_c}$$

Another important variation of the van der Waals EOS was introduced in 1976 by Peng and Robinson (PR-EOS) [33]. Improved density prediction was the main motivation of the authors which in general is superior in density predictions of reservoir fluid systems. Although this equation improves the liquid density prediction, it cannot describe volumetric behavior around the critical point. The Peng and Robinson EOS (equations 3-4) is perhaps the most popular and widely used EOS [41].

$$P = \frac{RT}{v_m - b} - \frac{a(T)}{v_m(v_m+b)+b(v_m-b)} \quad (3)$$

Where

$$a(T_c) = 0.45724\frac{(RT_c)^2}{P_c} \quad (4)$$

$$b = 0.07780\frac{RT_c}{P_c}$$

Schmidt and Wenzel [42] incorporated the acentric factor as the third parameter in the attractive term (equation 5) [41] as:

$$P = \frac{RT}{v-b} - \frac{a_c\alpha}{v^2+(1+3\omega)bv-3\omega b^2} \quad (5)$$

4.6 Three Parameter Equation of State

Redlich–Kwong (RK) cubic EOS have been proved to be very reliable tools in the prediction of phase behavior. Despite their good performance in compositional calculations, they usually suffer from weaknesses in the predictions of saturated liquid density [43]. A two-parameter EOS predicts the same critical compressibility factor, Z, for all substances while the inaccuracy of predicted volume at the critical point, not necessarily leads to unreliable volumetric data at all conditions, it demonstrates the inflexibility of two-parameter EOS for matching both the vapor pressure and volume. The inclusion of a third parameter relaxes the above limitation. Ashour et al [41] postulated that the third parameter is generally determined by employing volumetric data.

5. METHODOLOGY

The analysis of pressure depletion for a gas condensate reservoir in this work was done with the use of Eclipse 100 [44] and Eclipse 300 [44] reservoir simulators to generate production and pressure data. The simulator selected for use is a standard industry Black-oil and Compositional reservoir simulators, they are proven to be robust and reliable with many ancillary packages to facilitate data preparation and processing of results. The Compositional simulation model recognises that the reservoir is quite close to the critical point and thus represents the oil and gas phases as a multi-component mixture, at all temperatures and pressures. Each component (C_1, C_2, etc.) is tracked in the simulator. It also accounts for changes in the fluid behaviour and properties with changes in pressure in an isothermal environment.

The procedure for this study is outlined as follows:

- Data assembly and analysis (primarily aggregate data from existing gas condensate fields).
- Construction of a simulation model to accurately represent a gas condensate field/reservoir.
- Simulation of production and pressure data for analysis and further study.
- Interpretation of results to analyse and understand the effect of pressure depletion on well deliverability, condensate yield and condensate blockage. Also, the effect of condensate dropout on the relative permeability function is analysed.
- Sensitivity analysis on various EOS models, and modelling approach (compositional versus black oil) and comparison of results for various PVT observed data.

5.1 Data Assembly and Analysis

The model was built using data from existing gas condensate fields. The data includes fluid

PVT data (Figs. 5-7), saturation versus relative permeability curve (Figs. 8-9), porosity, permeability and well data. The EOS model used here is a derivative of the Peng-Robinson Equation of state and the Peng-Robinson correction parameter using laboratory PVT data. This equation of state is solved to obtain the Z-factors for the liquid and vapour phases and phase fugacities which are necessary for inter-phase equilibrium calculations and fluid densities (important for material balancing). Of the 3 solutions obtained for the Z-factor, the largest is taken for the vapour phase and the smallest for the liquid phase.

As shown in the figure 5 above the dew point pressure is 4800psia, average reservoir temperature is 320°F and initial reservoir pressure is 5400psia.

5.2 Reservoir Model Description

The model is a three-phase 3D model of a gas condensate reservoir initially above the dew point line. The simulation grid contains 648 active cells with the dimension 9 x 9 x 8 in the X, Y and Z directions (Fig. 10). The grid type used is the Block-centred Cartesian grid. This grid system averages reservoir properties at the centre of the grid cell. Block-centred geometry uses the DX, DY, DZ and TOPS keywords to specify the size of each grid cell in the X, Y and Z directions and the top of the reservoir respectively. The cells are rectangular and have horizontal upper and lower surfaces and vertical sides. The reservoir heterogeneity was captured by varying permeability in the X, Y and Z directions using the keywords PERMX, PERMY and PERMZ respectively. There are six components considered namely; C_1, C_3, C_{10}, C_{15}, CO_2 and N_2 in the primary base case model. The thickness of each cell in the X and Y and Z directions are 1200ft, 1000ft and 30ft respectively. Average cell porosity is 25% and net-to-gross is 1.0. Permeability varies in each layer, the ratio of vertical to horizontal permeability is 0.2.

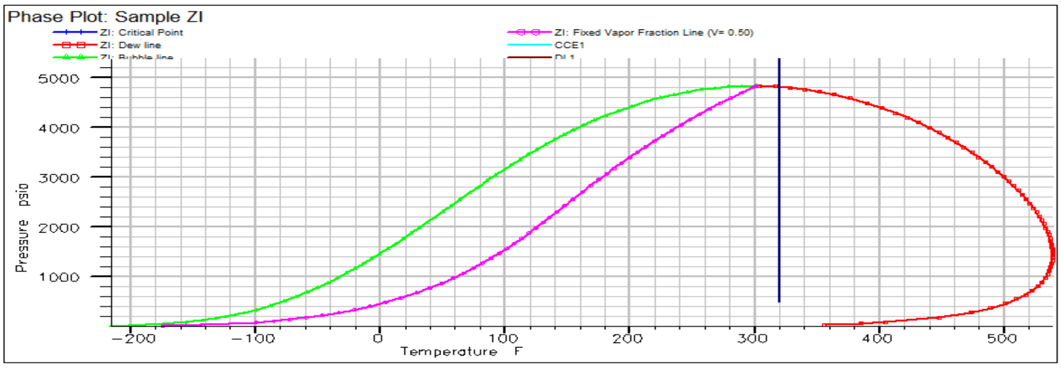

Fig. 5. Phase envelope for the gas condensate fluid sample generated in PVTi

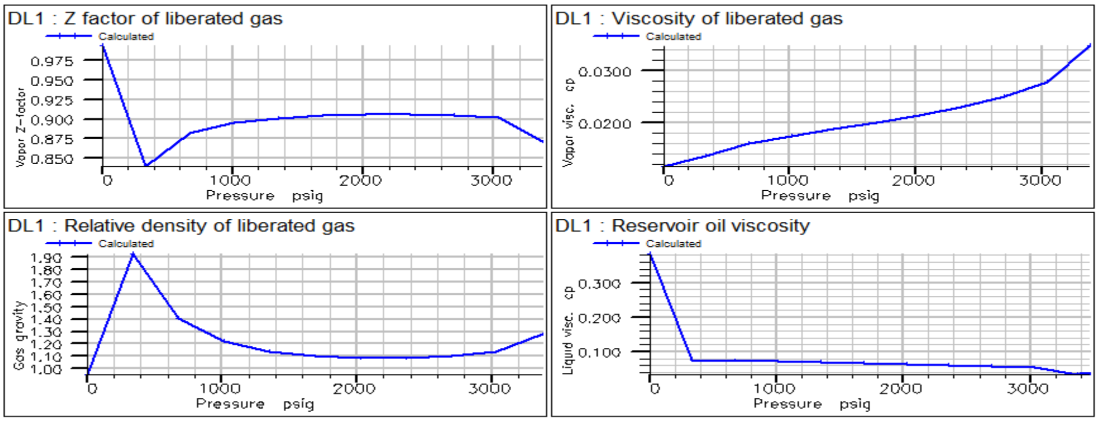

Fig. 6. Plot of gas properties against pressure generated from differential liberation experiments in PVTi

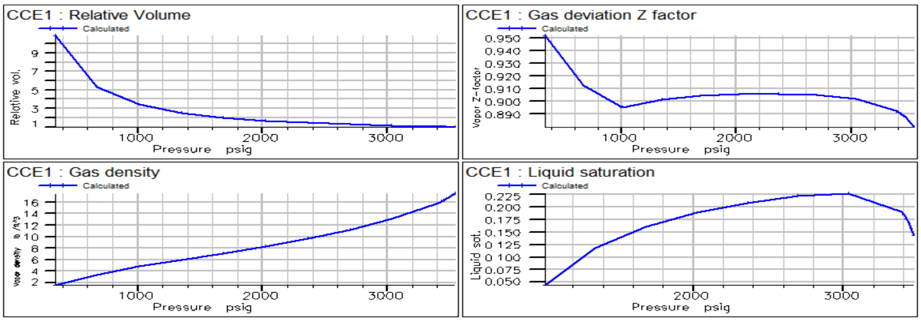

Fig. 7. Fluid properties characterization in EOS model generated from CCE experiment in PVTi

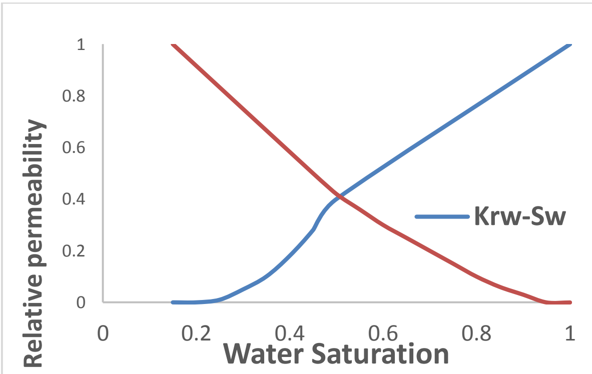

Fig. 8. Gas-Water relative permeability versus saturation function

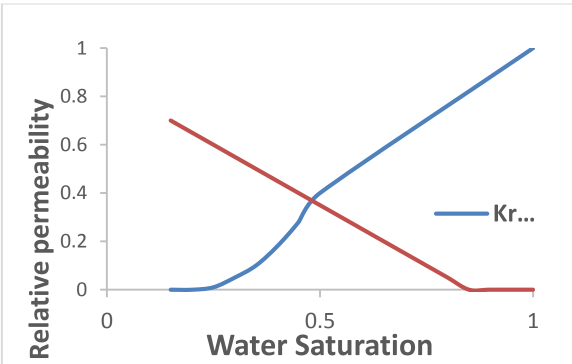

Fig. 9. Oil-water relative permeability versus saturation function

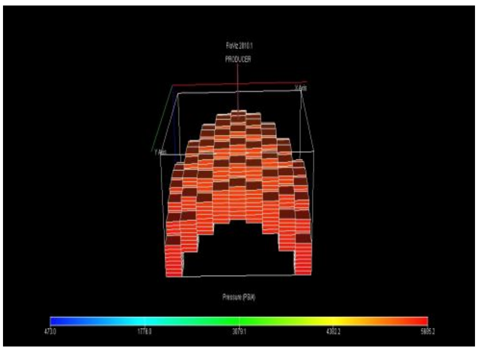

Fig. 10. Reservoir Grid

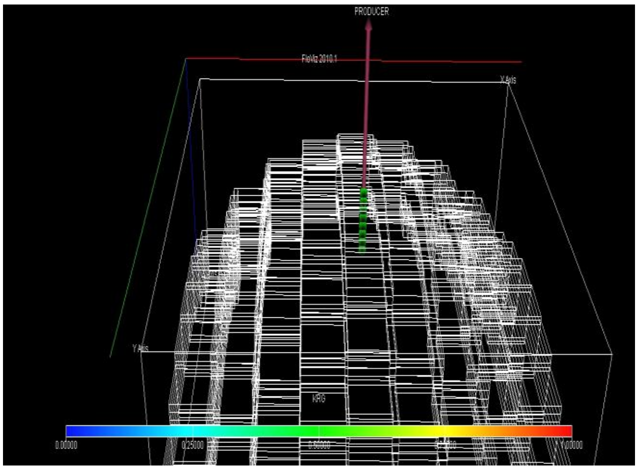

Fig. 11. Vertical well used within the skeletal grid structure

5.3 Well Model

The well in this model is a vertical well (Fig. 11) with a radius of 0.33ft.and zero skin. The equivalent grid-block radius is calculated in the reservoir simulator by Peaceman's formula.

The model contains one gas producer positioned at the centre of the reservoir controlled in bottom-hole pressure mode and regulated to produce 500,000Mscf/day of gas with a minimum BHP of 100psia. The produced fluids are separated at the surface in a 3-stage separation with varying pressure and temperature conditions.

6. RESULTS, ANALYSIS AND DISCUSSION

6.1 Black Oil Versus Compositional Modelling

The results obtained for the black oil and compositional models were compared and the plots are shown below (Figs. 12-12). Although the results were similar in trend, the values obtained were different with the results of the compositional simulation clearly more accurate and representative of the gas condensate reservoir.

The results indicate that the black oil modelling of gas condensate generates more optimistic results than the compositional modelling for the gas phase. However, the black oil model is still representative of the gas condensate because they generally produce the same trend and thus can be used as a quick test. Analysis of various case models show that the black oil gas condensate model shows more optimistic results for gas production and less optimistic results for condensate production with pressure depletion, than the compositional model. This is due to the fact that the compositional model accounts for the various components and their respective compositions which affects the phase behaviour of the fluid system, unlike the black oil model which represents the phases as one component. The black oil model simply accounts for the condensate production from the vaporized oil as one component, hence the tendency to under estimate condensate production. This can be seen in Fig. 13 where the compositional model produces a much higher estimation of the vaporized oil-gas ratio than the black oil. Ultimately, the quantity of reservoir volume produced affects the pressure profile and this can be seen in Fig. 14 as the pressure profile for the compositional model arrives at the minimum BHP earlier (13months) than the black oil model (20months) due to greater withdrawal at the same conditions.

6.2 Results and Analysis from Compositional Model

The results from Fig. 16 showed that gas production rate was maintained at 500,000Mscf/day until the minimum BHP of 100psia was reached, when it began to decline. Also at this same point, the condensate production rate and oil-gas ratio which had previously followed the same plot took different directions. The condensate production rate tailing off to zero due to insufficient drawdown for production. The oil-gas ratio was maintained relatively constant due to the lack of condensate production/drop out from the produced gas.

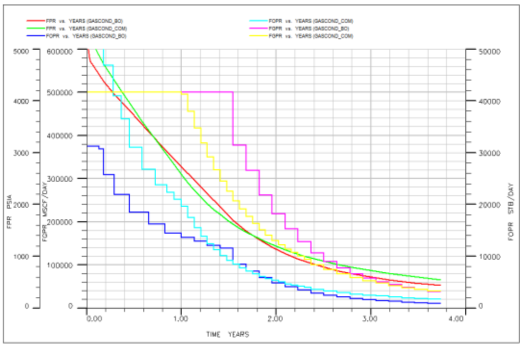

Fig. 12. Plots of average reservoir pressure, condensate production rate and gas production rate versus time

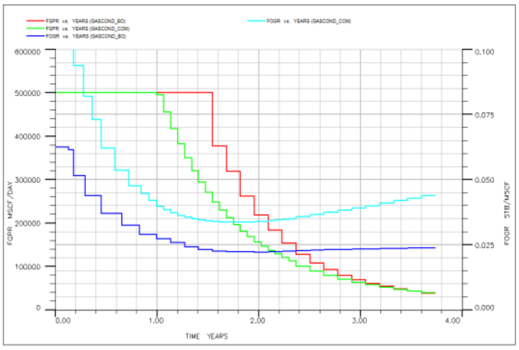

Fig. 13. Condensate-gas ratio and gas production rate versus time

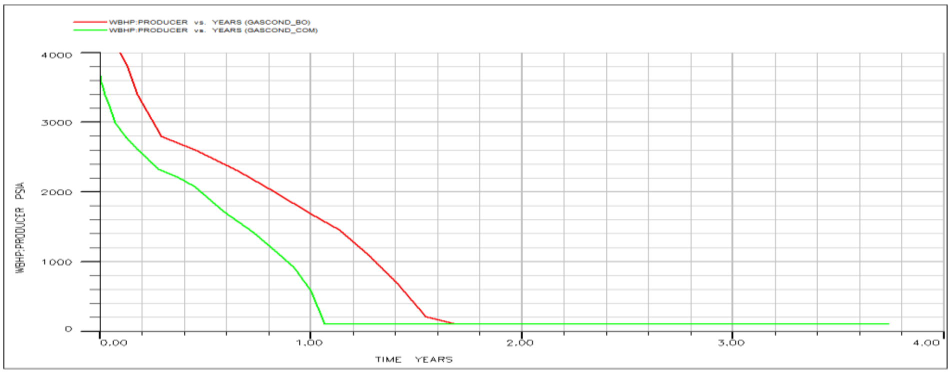

Fig. 14. bottom-hole pressure versus time (years)

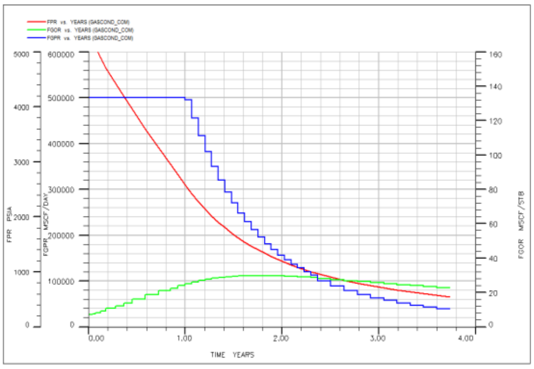

Fig. 15. Plot of average reservoir pressure, gas-oil ratio and gas production rate versus time

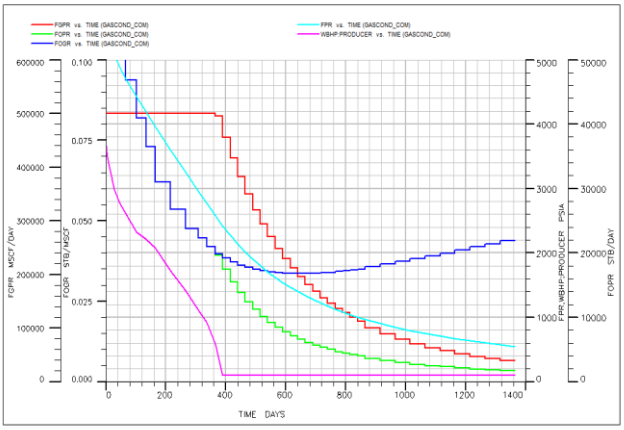

Fig. 16. Plot of bottom-hole pressure, condensate production rate, average reservoir pressure, gas production rate and condensate-gas ratio versus time

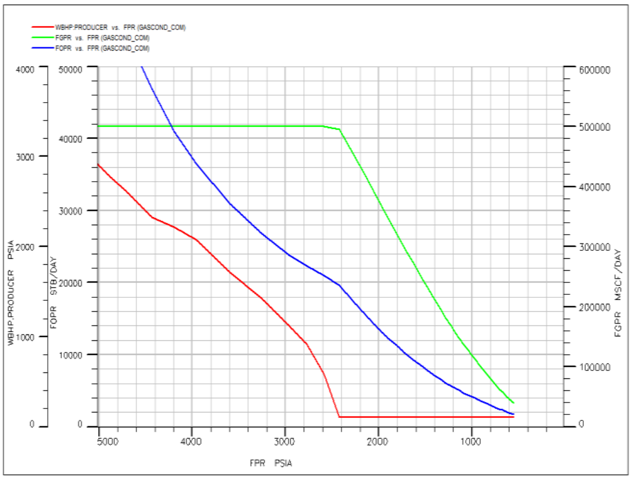

Fig. 17. Plot of bottom-hole pressure, gas production rate and condensate production rate versus average reservoir pressure

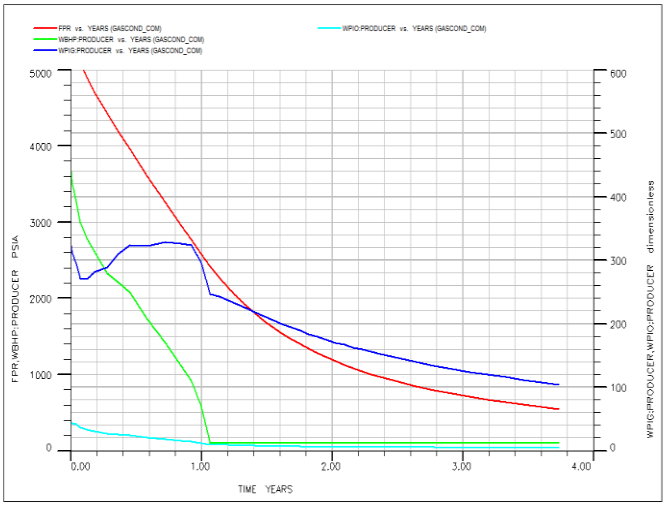

Fig. 18. Plot of condensate productivity index, gas productivity index, average reservoir pressure and bottom-hole pressure versus time

At the time the well BHP drops to the minimum value of 100psia which also coincides with a drop in oil productivity index to zero, the decreasing gas productivity index can be seen to take a gentler decline for the next 2.5 years of production. Which highlights the effect of condensate production on the gas deliverability of the well.

The gas productivity index as seen here was increasing steadily at pressures above the dew point after the initial stabilizing stage. On reaching the dew point, the gas productivity index curve can be seen to decrease over time (after 10 months). The post-dew point curve can be seen to have two different gradient lines. The first being at increasing condensate drop out and the second at decreasing drop out. The second gradient line can also be explained by the drop in the condensate production rate at the same time. This is due to the typical occurrence in gas condensate reservoir where below the dew point, condensate drop out/yield increases to a point, and then subsequently decreases due to a re-vaporizing of the liquid in the gas phase. This is confirmed in Fig. 19 where we see an increase in the OGR at around 1400 psia reservoir pressure (at approximately 2 years).

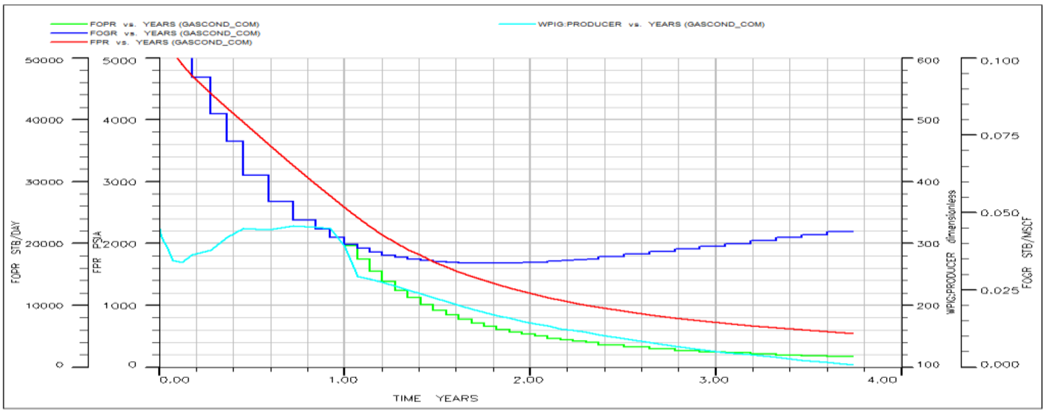

Fig. 19. Plot of condensate production, gas productivity index, average reservoir pressure, and condensate-gas ratio versus time

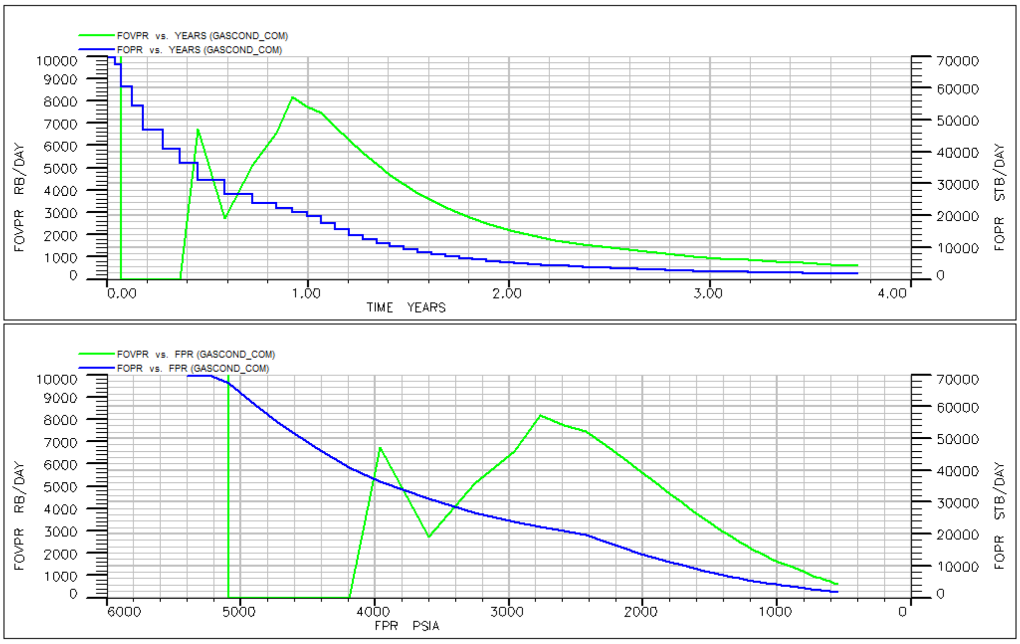

Fig. 20. Plot of Surface and Reservoir condensate production rate versus average reservoir pressure and time

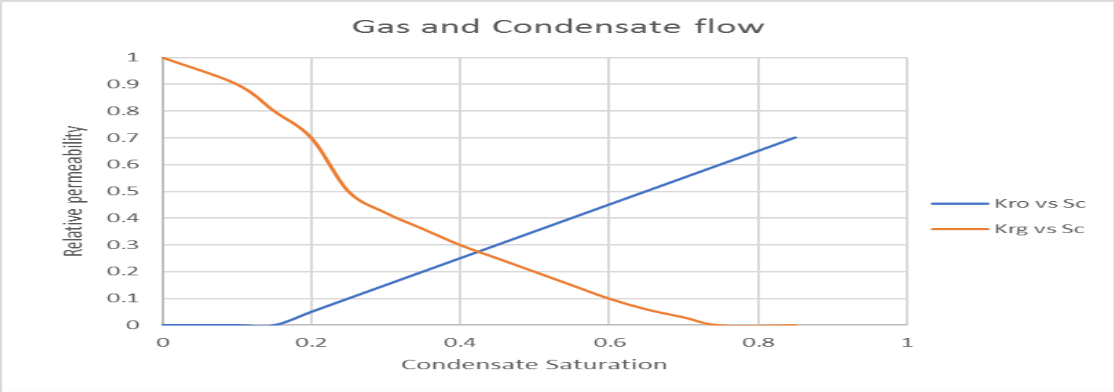

Fig. 21. Plot of oil and gas relative permeability versus condensate saturation

Fig. 20 showed both surface and reservoir oil production variation with time and average reservoir pressure. While oil production at the surface is evident from the onset, reservoir production of condensate is zero. This continues until the dew point pressure of 4800psia (as shown in the phase envelope in Fig. 5) when condensate starts to drop out of the gas phase. However, this condensate was still immobile until the saturation exceeded critical saturation when the condensate began to flow in the reservoir. This happened at around 4200psia (at about 5 months) as seen on the plot. The effect of condensate dropout on relative permeability is shown in Fig. 21. With increasing condensate saturation, particularly around the well bore, the gas relative permeability can be seen to decrease. This demonstrates the effect of condensate blockage around the well.

6.3 Comparison of Results using Different EOS

Comparing the results for the three different models using the Peng-Robinson 3-parameter (PR3), Soave-Redlich-Kwong 3-parameter (SRK3) and the Schmidt-Wenzel 2-parameter (SW2) Equations of state, a pattern can be shown.

From Fig. 22, the total gas production from the field can be seen to have similar results for all three EOS. However, the total field condensate production recorded were very distinct, with the PR3 model showing the highest estimate while the SW2 showed the lowest estimate. This highlights the limitation of the 2-parameter EOS models i.e. their inability to accurately predict liquid properties (density and saturation) and thus lower estimates of the vaporized oil in the gas phase, from which condensate emerges, and lower condensate production is predicted. PR3 and SRK3 on the other hand, compensate for this limitation with the introduction of a third parameter, the molar volume correction and thus record higher. This is also evident from the GOR plot, as the lower condensate production estimate (and OGR), the higher the GOR estimate.

The gas production rate and total volume is not particularly affected by the EOS model used. However, the gas deliverability is greatly affected (Fig. 23). The 2-parameter SW model shows much greater estimates of gas productivity index, compared to the PR3 EOS model for the first few years. Subsequently, the values become very similar due to generally reduced production activities at the latter stages when the well BHP reaches the minimum value of 100psia. The converse is true for the oil productivity index.

6.4 Comparison of Results using Base Case Model against Akpabio et al.'s and Shi's Models

The works of Akpabio et al. [4] and Shi [15] were analysed and their PVT data consisting of the various components (C1, C6 etc.), their compositions, molecular weight, acentric factors (where available) etc. was converted into a workable model in PVTi [44]. Complete Eclipse input files were created for both models with the models maintaining the same input data as the base case model in describing the reservoir rock properties (porosity, permeability, thickness, Area etc.), rock-fluid interaction characterisation (capillary pressure, saturation functions etc.), well information etc. but with a different PVT section to analyse the observed trends and to check consistency with theoretical expectations of gas condensate reservoirs.

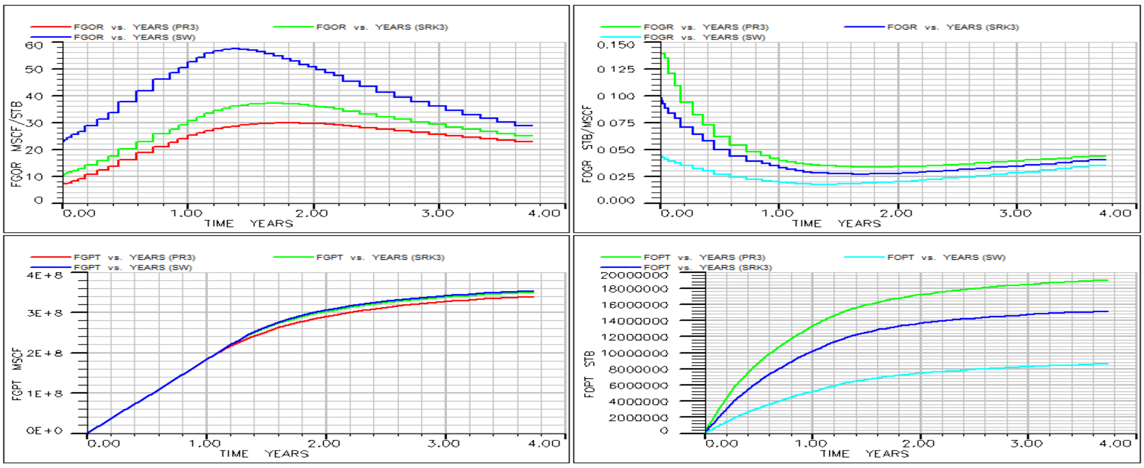

Fig. 22. Plot of vaporized condensate and dissolved gas ratios and total gas and condensate production versus time for the three EOS used

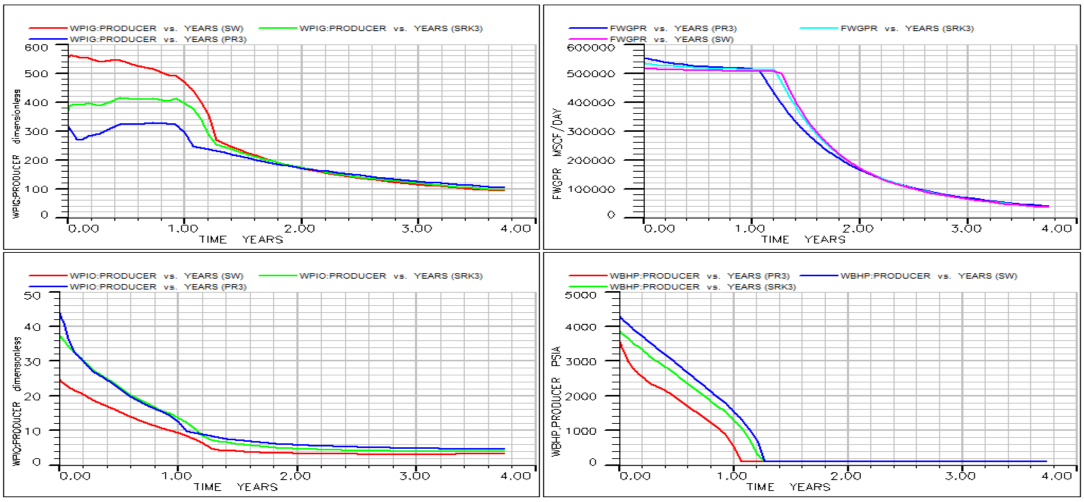

Fig. 23. Plot of gas and condensate productivity index, bottom-hole pressure and wet gas production rate versus time

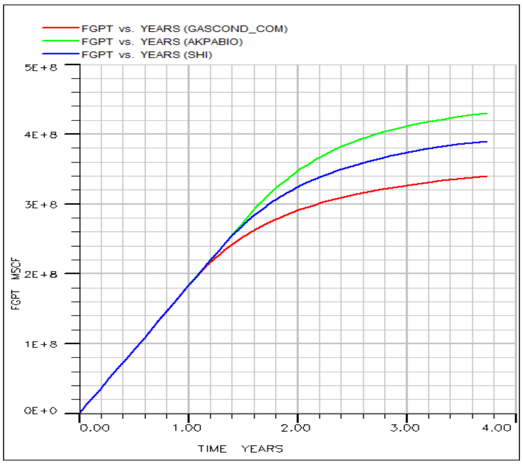

Fig. 24. Plot of total gas production for all three models against time (at the same initial average reservoir pressure)

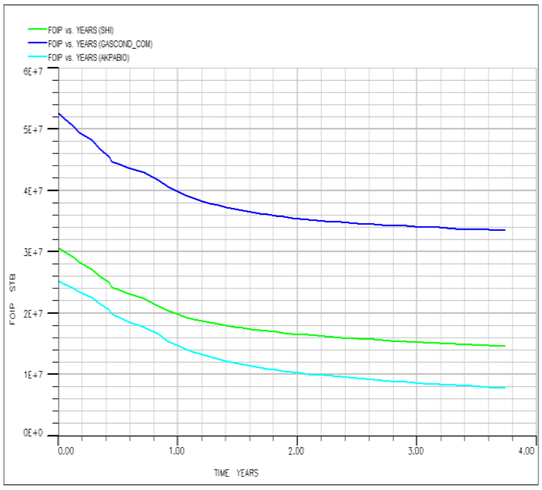

Fig. 25. Plot of condensate in place for all three models against time (at the same initial average reservoir pressure)

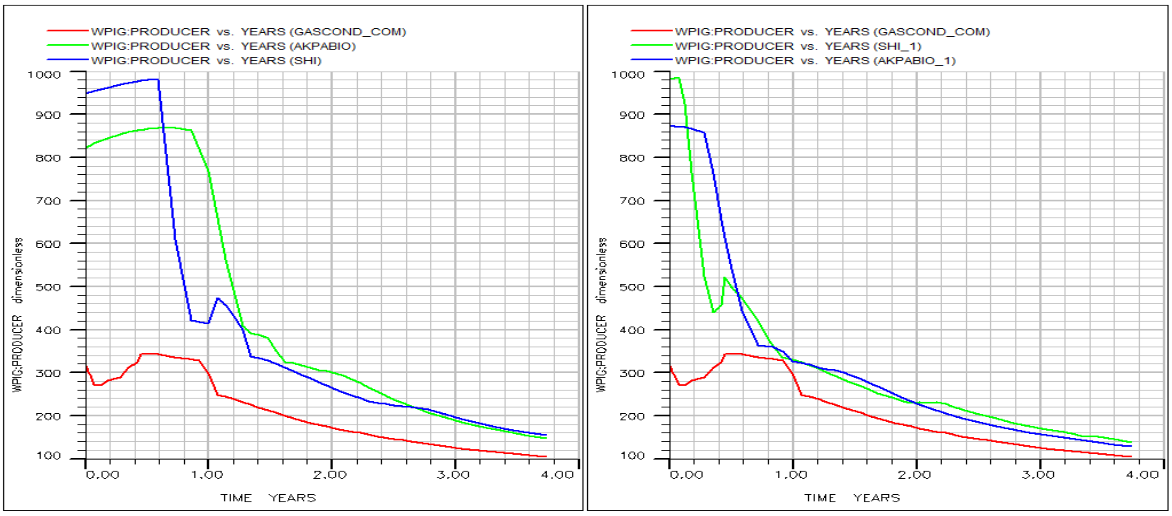

Fig. 26. Plot of gas productivity index against time for all three models at the same initial reservoir conditions (Pressure=5400psia) and at different initial reservoir conditions (Pressure=5400psia, Pressure=3500psia)

From the plot it can be seen that the cumulative gas production result for the base case model has the least value compared to the others. This is expected given that the phase envelope obtained for all PVT data show a closeness to the critical point (thus lower proportion of gas and consequently higher proportion of liquid). The phase envelope obtained for the Akpabio PVT data is farther away from the critical point than either of the other models and thus at similar reservoir and operating conditions, produces the highest amount of total gas.

The results show that for the same operating conditions and at the same initial reservoir pressure of 5400psia (Plot 1), the well gas productivity index for the base case model gives the lowest values while the values for Akpabio et al. [4] and Shi [15] are considerably higher. This is expected because the phase envelope profiles for the PVT data for all 3 models show that the base case model is closer to the critical point i.e. higher proportion of condensate which means lower proportion of produced gas than the other two models. Results from Plot 2 for all three models with different conditions of initial reservoir pressure (5400psia for the base case model and 3500psia for the models of Akpabio et al. [4] and Shi [15] show that the well gas productivity index for the base case model still has the lowest recorded values compared to the others, irrespective of the conditions. This confirms the value of fluid PVT characterisation and the influence on reservoir fluid behaviour and production.

For the results of Akpabio et al. [4] and Shi [15], we can see that at pressures below the dew point (2400psia and 2800psia, respectively) the condensate production recorded at the surface decreases. This is due to the effect of condensate drop out in the reservoir. However, the reservoir condensate production is still zero until the condensate saturation in the reservoir exceeds the critical saturation and begins to flow. All production recordings at both reservoir and surface conditions terminate at the minimum BHP of 100psia as seen in Fig. 26.

7. CONCLUSION

In line with the objectives of this work, the behavior of gas condensate reservoirs was analyzed from a compositional perspective and the study was done through theoretical and numerical simulation work.

The changes in the liquid and vapor phases, performance of a gas condensate reservoir in terms of production rate and index with condensate drop out and the effect of pressure depletion on relative permeability and well deliverability (productivity index) observed in this study are presented as follows:

- Analysis of various case models show that the black oil gas condensate model shows more optimistic results for gas production and less optimistic results for condensate production with pressure depletion, than the compositional model.
- The productivity of gas condensate reservoirs can be improved by the use of an optimum production strategy that can keep the average reservoir pressure higher than the dew point pressure for longer, thus preventing drop out of heavier components around the well bore which causes a blockage.
- Identifying the average reservoir pressure at which the condensate drop out will start to decrease after the initial decrease below the dew point will help to maximise the recovery of condensate which has a higher economic value than gas.
- Optimal results are derived in modeling gas condensate reservoirs using 3-parameter EOS (Peng-robinson, Redlich kwong etc.) which provide a molar volume shift to prevent an underestimation of liquid density and saturations and thus accurate condensate mass balancing.
- Higher BHP values produced less condensate banking and a smaller amount of heavy-component is trapped in the reservoir. The lower the producing rate, the lower the amount of heavy-component left in the reservoir.
- Gas productivity can be maximized with a proper producing strategy. The total gas production can be increased by lowering the BHP or optimizing the producing rate.
- Both relative permeability and absolute permeability have effects on condensate banking behavior through the influence of the mobility term.

COMPETING INTERESTS

Authors have declared that no competing interests exist.

REFERENCES

1. Ifeanyi S, Oyinkepreye O, Paul ALA, Efeoghene E, Charles O. Modelling the effect of composition change during condensate dropout in a horizontal gas well. International Journal of Applied Engineering Research ISSN 0973-4562. 2017;12(2):179-189.
2. Izuwa NC, Obah B, Appah D. Optimal gas production design in gas condensate reservoir. Paper SPE-172453-MS presented at the SPE Nigeria Annual International Conference and Exhibition, Lagos, Nigeria; 2014.
3. Izuwa N, Ogbunude BC. Parametric study of enhanced condensate recovery of gas condensate reservoirs using design of experiment. J Pet Environ Biotechnol. 2015;7:1.
4. Akpabio JU, Isehunwa SO, Akinsete OO. PVT Fluid sampling, characterization and gas condensate reservoir modelling. Advances in Research. 2015;5(5):1-11.
5. Crafts BC, Hawkins MS. Applied Petroleum Reservoir Engineering; 1991.
6. Kerunwa A, Uchuebuacor C. Optimization of condensate recovery using gas recycling technique. Petroleum and Coal. 2015;57(5):565-575.
7. Fan I, Harris B, Jamaluddin A, Kamath J, Mott R, Whitson C. Understanding Gas Condensate reservoirs. Oilfield Review. 2005;17(4):14–27.

8. Aaditya K. Effect of reservoir and completion parameters on production performance in gas condensate reservoirs. Master Thesis, Department of Chemical and Biomolecular Engineering, University of Houston; 2014.
9. Adriana POC. New correlations for dew point, specific gravity and producing yield for gas condensates. Master Thesis, Petroleum Engineering, Graduate A and M University; 2002.
10. Vo HA, Horne RN. Experimental study of composition variation during flow of gas-condensate. Paper presentation at the SPE Annual Technical Conference and Exhibition held in Houston, Texas, USA; 2015.
11. Zhang HR, Wheaton RJ. Condensate banking dynamics in gas condensate fields: Compositional changes and condensate accumulation around production wells. Presented at the SPE Annual Technical Conference and Exhibition, Dallas, Texas, 1-4 October. SPE-62930-MS; 2000
12. Shi C, Horne RN. Improved recovery in gas-condensate reservoir considering compositional variations. Presented at the SPE Annual Technical Conference and Exhibition, Denver, Colorado, USA, 21-24 September. SPE-15786-MS; 2008.
13. Seah YH, Gringarten AC, Giddins MA, Burton K. Optimising recovery in gascondensate reservoirs. Presented at the SPE Asia Pacific Oil and Gas Conference, Adelaide, Australia, 14-16 October. SPE-171519-MS; 2014.
14. Amani M, Nguyen NT. An Overview of methods to mitigate condensate banking in retrogade gas reservoirs. Advances in Petroleum Exploration and Development. 2015;9(2):1-6.
15. Shi C. Flow behaviour of gas condensate wells. PhD Dissertation, Department of Energy Resources Engineering, Stanford University; 2009.
16. Rajeev RL. Well testing in gas condensate reservoirs. Master’s Thesis, Department of Petroleum Engineering, Stanford University; 2003.
17. Kanatbayev M. Gas condensate field performance theory versus practice. Master’s Thesis, Faculty of Science and Technology, University of Stravanger; 2012.
18. Bradley HB, Fred WG, Mohamed M, Aziz SO, Lewis LR, Philip SS, Gerry LS. Petroleum engineering handbook; 1992.
19. El-Banbi AH, McCain WD. Investigation of well productivity in gas-condensate reservoirs. presented at SPE/CERI gas technology symposium, calgary, Canada, 3-5 April. SPE-59773-MS; 2000.
20. Almehaidab RA, Al-Khanbash AS, Ashour L, Ali MA. A systematic approach to enhance the quality of PVT experimental data for Gas condensate reservoir evaluation. Journal of the Japan Petroleum Institute. 2003;46(3):203-209.
21. Whitson CH, Øiving F, Tao Y. Gas condensate PVT-what’s really important and why? Paper presented at the IBC Conference “Optimisation of Gas Condensate Fields”, London, Jan. 28-29, Cumberland Hotel; 1999.
22. Keith SC. Simulation of gas condensate reservoir performance. SPE-10512.SPE Intercomp Resource Development and Engineering; 1985.
23. Coats KH, Thomas LK, Pierson RG. Compositional and black oil reservoir simulation. SPE 29111. This paper was prepared for presentation at the 13th SPE Symposium on Reservoir Simulation held in San Antonio, TX, U.S.A; 1995.
24. Hamoodi AN, Abed AF, Firoozabadi A. Compositional modelling of two-phase hydrocarbon reservoirs first presented as SPE 36244 at the 7th Abu Dhabi International Petroleum Exhibition and Conference, in Abu Dhabi, UAE; 1996.
25. Øivind F, Kameshwar S, Curtis HW. Guidelines for choosing compositional and black-oil models for volatile oil and gas-condensate reservoirs. SPE 63087. This paper was prepared for presentation at the 2000 SPE Annual Technical Conference and Exhibition; 2000.
26. Fevang Ø, Whitson CH. Modeling Gas Condensate Deliverability. SPE Paper 30714, presented at the SPE Annual Technical Conference & Exhibition held in Dallas, U.S.A; 1995
27. Ahmed HE, Forrest JK, Fan L, McCain WD Jr. Producing rich-gas-condensate reservoirs--case history and comparison between compositional and modified black-oil approaches. SPE 58988 Schlumberger Holditch-Reservoir Technologies Presentation at the 2000 SPE International Petroleum Conference

and Exhibition in Mexico held in Villahermosa; 2000.
28. Sashay R, Edison M, Mohamed B. A review of the equations of state and their applicability in phase equilibrium modeling. International Conference on Chemical and Environmental Engineering (ICCEE'2013) April 15-16, Johannesburg (South Africa); 2013.
29. Duan Z, Hu J. A New cubic equation of state and its applications to the modeling of vapor-liquid equilibria and volumetric properties of natural fluids. Geochimica et Cosmochimica Acta, 2004;68(14):2997–3009.
30. van der Waals JD. Over de continuiteit van den gas- en vloeistoftoestand (On the Continuity of the Gaseous and Liquid States) (doctoral dissertation). Universiteit Leiden; 1873.
31. Redlich O, Kwong JNS. On the thermodynamics of solutions. An Equation of State. Fugacities of Gaseous Solutions". Chemical Reviews. 1949 ;44(1):233–244.
32. Soave G. Equilibrium constants from a modified redlich-kwong equation of state, to high temperatures and high pressures. Ber. Bunsenges. Phys. Chem. 1972;90:780-789.
33. Peng DY, Robinson DB. A new two-constant equation of state. Industrial and Engineering Chemistry Fundamentals. 1976;15:59-64.
34. Carnahan NF, Starling KE. Equation of state for nonattracting rigid spheres. Journal of Chemical Physics. 1969;51:635-636.
35. Guggenheim EA. Variations on van der waals' equation of state for high densities, Mol. Phys. 1965;9:199-200.
36. Boublik T. Statistical thermodynamics of nonspherical molecule fluids. Ber. Bunsenges, Phys. Chem. 1981;85:1038-1041.
37. Wei YS, Sadus RJ. Equations of state for the calculation of fluid-phase equilibria, AIChE J. 2000;46:169-195.
38. Chen SS, Kreglewski A. Applications of the augmented van der waals theory of fluids.: Part I. Pure Fluids. Phys. Chem. 1977;81:1048-1052.
39. Christoforakos M, Franck EU. An equation of state for binary fluid mixtures to high temperatures and high pressures. Ber. Bunsenges. Phys. Chem. 1986;90:780-789.
40. Heilig M, Franck EU. Calculation of thermodynamic properties of binary fluid mixtures to high temperatures and high pressures, ber. Bunsenges. Phys. Chem. 1989;93:898-905.
41. Ashour I, Nabeel A, Amin F, Gholamreza V. Applications of equations of state in the oil and gas industry. Thermodynamics – Kinetics of Dynamic Systems. 2011;165-178.
42. Schmit G, Wenzel H. A modified van der Waals type equation of state, Chem. Eng. Sci. 1980;35:1503-1511.
43. Mousavian S, Mousavian F, Rashidabad N. Modification of RK equation of state for liquid and vapour of ammonia using genetic algorithm. World Academy of Science, Engineering and Technology International Journal of Chemical and Molecular Engineering. 2014;8:1.
44. Eclipse 100, Release; 1998a.

Peer-review history:
The peer review history for this paper can be accessed here:
https://www.sdiarticle4.com/review-history/70535